Faraday Discussions

Accepted Manuscript

This manuscript will be presented and discussed at a forthcoming Faraday Discussion meeting. All delegates can contribute to the discussion which will be included in the final volume.

Register now to attend! Full details of all upcoming meetings: http://rsc.li/fd-upcoming-meetings

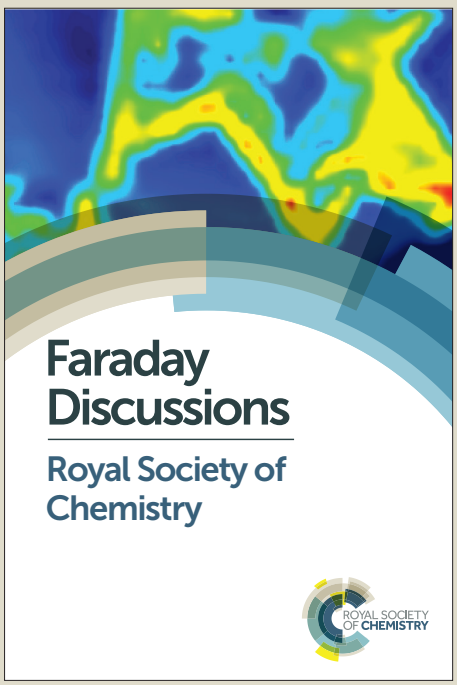

This is an *Accepted Manuscript*, which has been through the Royal Society of Chemistry peer review process and has been accepted for publication.

Accepted Manuscripts are published online shortly after acceptance, before technical editing, formatting and proof reading. Using this free service, authors can make their results available to the community, in citable form, before we publish the edited article. We will replace this *Accepted Manuscript* with the edited and formatted *Advance Article* as soon as it is available.

You can find more information about *Accepted Manuscripts* in the Information for Authors.

Please note that technical editing may introduce minor changes to the text and/or graphics, which may alter content. The journal's standard Terms & Conditions and the Ethical guidelines still apply. In no event shall the Royal Society of Chemistry be held responsible for any errors or omissions in this *Accepted Manuscript* or any consequences arising from the use of any information it contains.

ROYAL SOCIETY OF CHEMISTRY

www.rsc.org/faraday_d

ARTICLE

Nanocapillary Electrokinetic Tracking for Monitoring Charge Fluctuations on a Single Nanoparticle

Sanli Faez,[a†] Sela Samin,[b] Dashdeleg Baasanjav,[a] Stefan Weidlich,[c, d] Markus Schmidt,[d] Allard P. Mosk[a]

We introduce *nanoCapillary Electrokinetic Tracking* (nanoCET), an optofluidic platform for continuously measuring the electrophoretic mobility of a *single* colloidal nanoparticle or macromolecule in vitro with millisecond time resolution and high charge sensitivity. This platform is based on using a nanocapillary optical fiber in which liquids may flow inside a channel embedded inside the light-guiding core and nanoparticles are tracked using elastic light scattering. Using this platform we have experimentaly measured electrophoretic mobility of 60-nm gold nanoparticles in an aqueous environment. Further, using numerical simulation, we demonstrate the underlying electrokinetic dynamics inside the nanocapillary and the necessary steps for extending this method to probing single biomolecules, which can be achieved with existing technologies. This achievement will immensely facilitate the daunting challenge of monitoring biochemical or catalytic reactions on a single entity over a wide range of timescales. The unique measurement capabilities of this platform pave the way for a wide range of discoveries in colloid science, analytical biochemistry, and medical diagnostics.

Introduction

More than a century after Robert Millikan had reported on measuring the elementary charge, his method is still being used for experiments such as high precision detection of fractional charges at ambient conditions [1] or single charging events on an optically-trapped colloid particle in an apolar solvent [2]. In this method, by observing the drift velocity of a particle forced by an external electric field one obtains its electrical mobility, which has usually a well-defined relation with the net charge of the particle. In parallel measuring electrophoretic mobility has become one of the most common methods in analytical (bio)chemistry and colloid science. The electrophoretic mobility (drift velocity in a viscous medium under application of external electric field) of proteins and other macromolecules is a very sensitive indicator of their internal charge state, their interaction with the surrounding environment, and their hydrodynamic radius. As such, it has been used for sorting a mixture of macromolecules [3] or studying their conformational changes due to chemical reactions or physical adsorption to other molecules. However, common electrophoresis measurement techniques are based on measuring ensembles. In an ensemble measurement, the observation of intermediate states is often impossible because of averaging over unsynchronized and inhomogeneous processes.

Single particle measurements, on the contrary, are not prone to disturbance by impurities, which can be singled out in data analysis. Furthermore, such measurements can be repeated as many times as necessary for collecting reliable and informative statistics. In other words, when the physicists' granular view of a reaction on a single particle is reconstructed by a direct measurement, the characteristic kinetics and thermodynamics of the reaction is no more obscured by material inhomogeneity or stochastic dynamics over the metastable intermediate states. Important chemical reactions, such as photo-catalysis or enzyme-catalysis, involve multiple steps of largely differing timescales. Furthermore, their reaction rates can be heterogeneous within an ensemble of catalyst particles and can even vary over time for a single catalyst particle. In principle, there is no

a. Debye Institute for Nanomaterials Research, Center for Extreme Matter and Emergent Phenomena, Utrecht University, Princetonplein 5, 3584CC Utrecht, The Netherlands.
Email: s.faez@uu.nl
b. Institute for Theoretical Physics, Center for Extreme Matter and Emergent Phenomena, Utrecht University, Princetonplein 5, 3584CC Utrecht, The Netherlands
c. Heraeus Quarzglas GmbH and Co. KG, 63450 Hanau, Germany
d. Leibnitz Institute of Photonic Technology, Albert-Einstein-Str. 9, 07754, Jena, Germany

fundamental barrier for studying a full chain of chemical reactions on a single molecule or nanoparticle through monitoring its electrophoretic mobility, if (and that is indeed a big if) one could track the single molecule motion both on the shortest necessary timescales and as long as the reaction is complete. In other words, if one could perform Millikan's experiment on objects as small single molecules, she or he could visualized reaction kinetics of that single object. In such a measurement, one can directly "watch" the intermediate steps of a reaction as they happen.

The single most challenging step for mobility measurement at this small scale on a single nanoparticle is tracking its motion with sufficient spatial and temporal resolution. On these criteria, optical methods generally score much higher than all-electronic techniques. The optical signal (for example scattering intensity) from sub-wavelength particles, however, decreases steeply as the particle size gets smaller. Very recently, we have demonstrated a new particle tracking method that provides the necessary sensitivity and speed for tracking sub-20-nm particles [4]. In this article we report on building a single particle optical capillary electrophoresis device based on that achievement. We dub this technique nanoCapillary Electrophoretic Tracking (nanoCET).

We present the details of our experimental setup and report the first measurements of electrophoretic mobility on a single particle in this platform with ms time resolution. As a typical colloidal particle we perform these measurements on a single gold nanoparticle of 60-nm in diameter in an aqueous environment, using the nanoCET technique. We explain some of our observations by comparing the measurements with numerical simulations using the finite element method. Based on these simulations, we write down the necessary follow-up steps for extending this method to probing single biomolecules.

Experimental

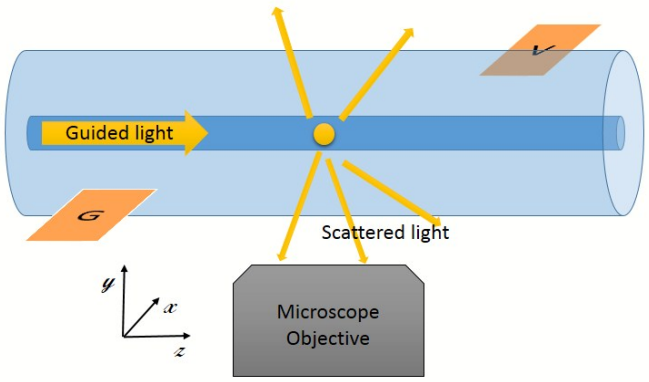

Figure 1: Schematic representation of the experimental conditions. Electrophoretically actuated thermally diffusing particles are tracked inside the liquid-filled core of a nanocapillary optical fiber. The electric field for actuation is generated by metal electrodes placed outside the fiber as depicted.

We have used nanofluidic optical fibers, which were previously introduced in [4], for visualizing the motion of nanoparticles inside the liquid. In these single-mode step-index fibers a hollow channel of 600 nm in diameter is embedded concentric to the light guiding doped-silica core. The channel can be filled with liquid containing the nanoparticles. Laser light is coupled into the fiber and the elastically scattered light is detected from the side of the fiber. The particle positions are imaged using the elastically scattered light from the fiber-core through a home-built microscope with an overall magnification of 100X connected to a high-speed sCMOS camera (Orca Flash4.0). Recorded sequences of images are processed for tracking the particles similar to the method presented in [4]. For the measurements reported here, we have additionally placed two micro-electrodes in-plane and orthogonal to the optical fiber as sketched in Fig. 1. The width of each electrode is 100 µm and the tip-to-tip distance between the electrodes is roughly 600 µm. The electrodes were connected to an alternating high-voltage amplifier ($|V - G| < 200$ Volts) which was fed by an alternating square waveform of frequency ν.

Gold nanoparticles (BBI-solutions) of 60 nm in diameter suspended in water were inserted into the nanocapillary of 50 mm length. The suspension was taken directly from the bottle provided by the manufacturer without any extra purification step. For each measurement, between 1 to 10 particles were visible inside the field of view of 200 µm from the center of the fiber with a signal to noise ratio of better than 100. Light at a vacuum wavelength of 670 nm from a diode laser (ventus, Laser Quantum) is coupled into the core of the fiber. The coupled intensity inside the fiber is estimated to be around 5 mW resulting in a net scattering signal of higher than 50 million electronic counts per second from each nanoparticle on the camera. This signal provides a localization accuracy of 60 nm for the center of the particle along the fiber axis, at the highest measurement rate and considering the sub-optimal point spread function of the imaging optics. Additional to the Brownian motion, the particles are driven back and forth under the influence of the alternating potential applied to the electrodes with a square waveform using a function generator and a low-noise amplifier. The particle tracks are recorded at a frame rate of 2 kHz for driving frequencies between 1 to 200 Hz.

To present a typical measurement, the velocity of a single particle as a function of time is plotted in Fig. 2 under actuation at 50 Hz. The particles oscillates synchronously with the alternating electric field. The average speed of the particle in the first millisecond of each period is roughly 30 µm/s. Deviation from the average is mainly due to Brownian motion. We observed no long term change in the

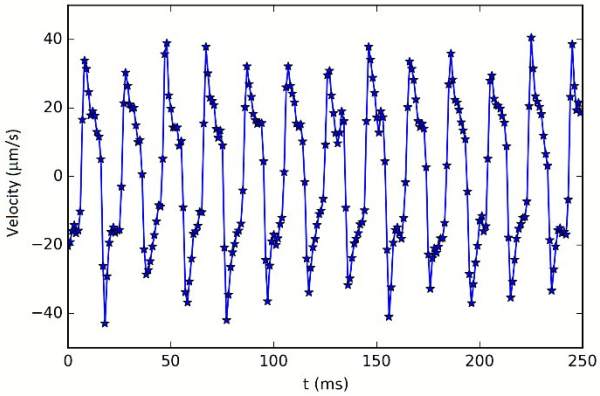

Figure 2: Drift velocity of a 60-nm gold nanoparticle inside the capillary under actuation by external electric field with a square waveform alternating at 50 Hz. The peak to peak variations are due to Brownian motion.

particle response even after tens of minutes, indicating the stability of the experimental conditions.

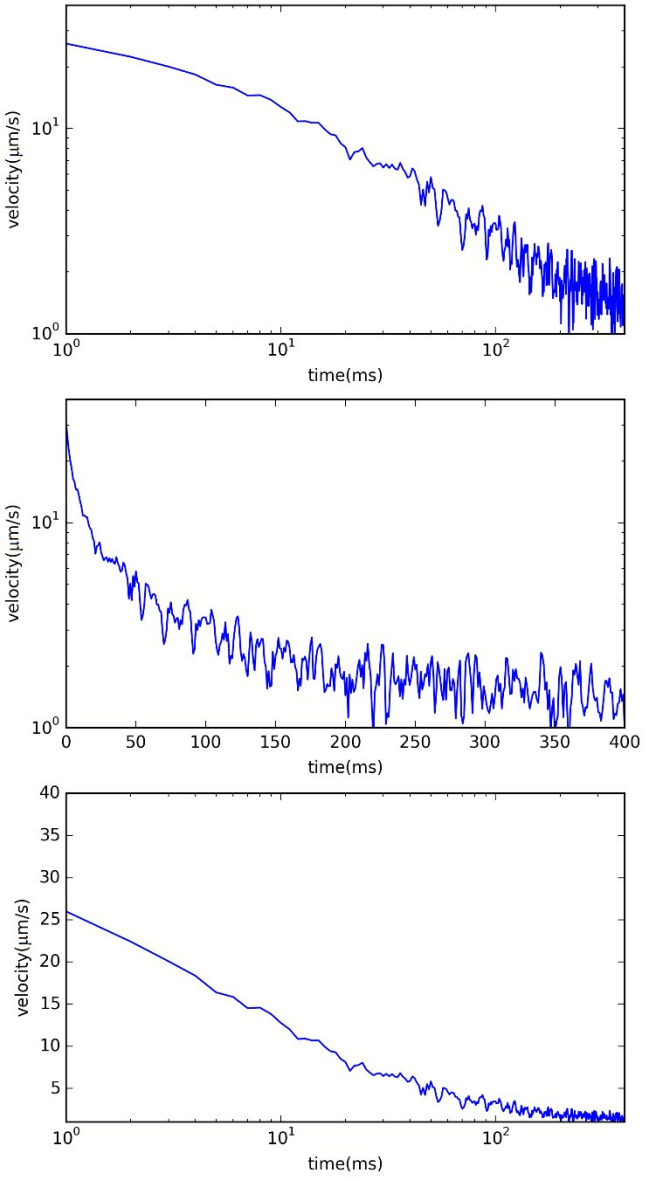

Figure 3: The average drift velocity of a single particle under constant applied potential decaying as function of time. The values are averaged over 10 cycles. Each panel show the same data with a different scaling on the axes. The decay behaviour is clearly not of a single exponential type.

The particle speed reduces to half its peak value 10 ms after the start of each period. This behavior is attributed to the restructuring of the double layer inside the capillary, which screens the electric field.

The electrophoretic dynamics of the particle and the surrounding ions are best visible in the tracks recorded at low driving frequency (Fig. 3). At the start of each cycle, particles move at an average drift velocity of 30 μm/s. The drift velocity decreases as the solvent ions reorganize to shield the electrostatic field inside the channel. After t = 100 ms through one cycle the particle displacement due to external field is undistinguishable from Brownian movements, but averaging over many cycles demonstrates persistence of nonzero average drift up to at least 500 ms. This curve is plotted in Fig. 3 for different combinations of the axis scaling. This decrease in drift velocity is clearly not behaving like a single exponential.

To determine the single particle mobility, and hence the charge of the particle from the drift velocity, we need to know the electrostatic field and the fluid velocity inside the channel. For this analysis, we need to know the influence of the electro-osmotic flow of the surrounding liquid and also separate the time dependence of the electrostatic field at the position of the particle due to ion screening dynamics. To this end, we have used finite element modelling to simulate the ion movement in a geometry that resembles our experimental conditions, but is smaller in size to make the computation tractable.

Modelling

The electrokinetic flow inside the capillary is described within the well-established framework of the Poisson-Nernst-Planck (PNP) equations [5] for the dynamics of point-like ions in combination with the Stokes equations for the fluid dynamics, assuming that $Re \ll 1$, where Re is the Reynolds number. The equations were solved using the finite-elements software COMSOL Multiphyiscs (v5.2). A schematic illustration of the computational domain is shown in Fig. 4. In order to make calculations in long capillaries computationally

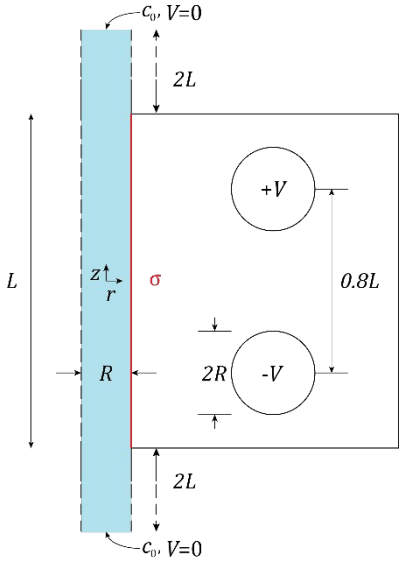

Figure 4: Schematic illustration of the computational domain in the numerical calculations. A charged capillary of radius R and length L is embedded in a silica matrix and connected to two large electrolyte reservoirs. Two ring electrodes with voltages $\pm V$ mimic the experimentally applied external field. See text for values of dimensions and other parameters. The illustration in not drawn to scale due to the large aspect ratio of the capillary.

feasible, we take advantage of the system symmetry and set-up a 2D cylindrical coordinate system (r, z). At the origin, we place a long cylindrical capillary with length $L = 10$ μm and radius $R = 0.2$ μm, connected at each end to a cylindrical material reservoir of length $2L$ and the same radius R. At the reservoir edges we set the electrostatic potential to zero, the salt concentration to c_0 and the total fluid stress to zero, in order to mimic a bulk fluid at rest. At $r = 0$ we impose symmetry boundary conditions while for the solid walls at $r = R$ we impose zero flux of the ionic species and the no-slip boundary condition for the fluid. The reservoir walls are insulating (zero displacement field) while the capillary wall carries a constant

charge density $\sigma = 6.1 \times 10^{-4}$ C/m², typical of a glass water interface [5]. The capillary is also surrounded by a silica matrix in which two oppositely-charged metal ring electrodes with a radius R are embedded. The electrodes are positioned at $(10R, \pm 0.4L)$. These electrodes model the spatially non-uniform applied external field in the experimental set-up and their potential $\pm V$ is set such that the generated electric fields are similar in magnitude to those in the experiment.

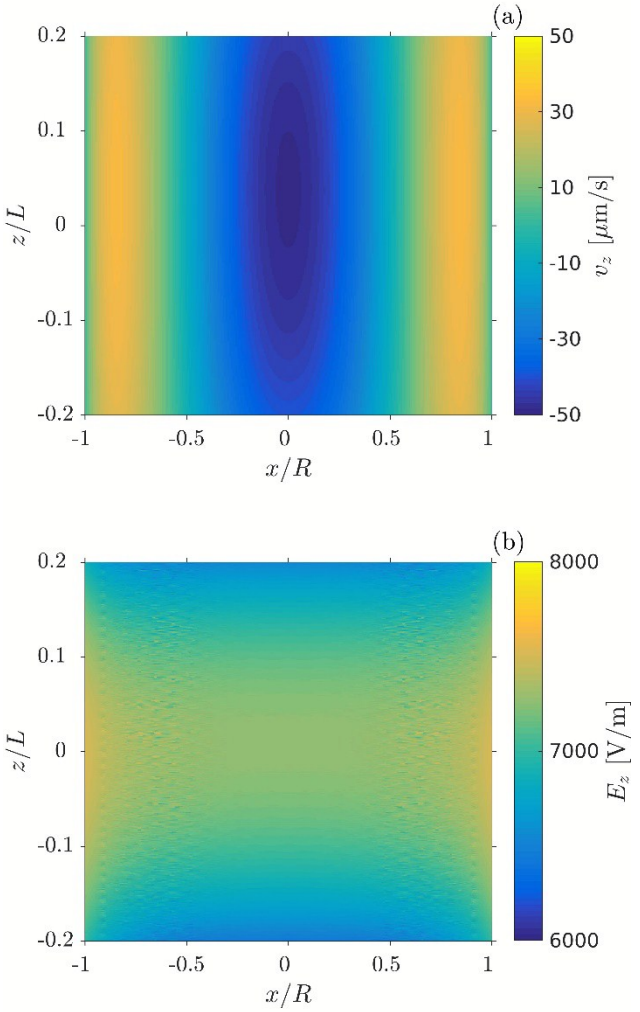

Figure 5: (a) The axial component of the fluid velocity and (b) the axial component of the electric field in the x-z plain at time $t = 0.03$ ms after the reversal of a voltage on the electrodes. The bulk salt concentration is $c_0 = 0.1$ mM. Here and in other figures we used the properties of water at 298 K for the solution inside the capillary, those of silica for the surrounding medium, and both cations and anions have a diffusion constant $D = 10^{-9}$ m²/s.

We start modelling from an equilibrated system under an external field where the electrodes' potential is $V = \pm 3$ V. In this state, a relaxed diffuse double-layer of ions with a characteristic thickness λ_D, the Debye length, is formed at the capillary wall, and the fluid is quiescent. We then abruptly reverse the electrodes' potential, $V \to -V$, following the square-wave function used in the experiments. The ions must then rearrange according to the new external field leading to an electro-osmotic flow in the capillary as they drag the fluid with them. Eventually, a new diffuse layer of ions will reform and the electric field will be screened. During this dynamic process, however, the field outside the double–layer is significant.

A snapshot of the resulting flow and electric field in the axial direction, shortly after the application of the voltage step, is presented in Fig. 5. Clearly, a complex electro-osmotic flow develops inside the capillary, with the axial component of the velocity v_z presented in Fig. 5(a) showing a change of sign at an intermediate distance from the capillary wall. Nevertheless, v_z is rather uniform in the axial direction and since $\gg R > a$, the diffusing colloidal particle only experiences the velocity gradients in the radial direction. We calculated the average velocity (averaged over the capillary cross-section) $\langle v_z \rangle$ for $z = 0$ in Fig. 5(a) and found that it does not vanish but is small, about 0.15 times the maximal velocity at $r = 0$. In contrast, Fig. 5(b) shows that the axial electric field E_z is uniform both axially and radially, especially at the capillary center. Assuming that the small particle does not disturb the flow substantially, we conclude that the particle experiences a uniform external electric field, parallel to the capillary axis, but also a variable local flow. On the measurement timescale of 1 ms, however, the particle traverses randomly the whole cross section of the channel, due to Brownian motion, and the net influence of this drag will be averaged out. We expect this net flow in the capillary to be much smaller for the experimental conditions because the channel is 3 orders of magnitude longer than the simulated model.

To characterize the dynamics of the particle environment, we plot in Fig 6 the time dependence of the axial velocity and electric field at the pore center for various salt concentrations. Notice that the simulation can access short time scales where the velocity at the pore center is very large. Both the velocity and electric field decay exponentially except for $c_0 = 0.02$ mM, where there is a distinct long tail. The relaxation time is slower for lower salt concentrations, but is short compared to experiments, being of the order of 0.1-1 ms for low values of c_0. This discrepancy is attributed to the limitation of short capillaries in the simulations. Analysis of diffuse charge dynamics by many authors [6-8] has shown that the primary time scale that controls bulk field screening by electrodes is $\tau = \lambda_D l/D$, where D *is* the diffusion constant of the ions and l is the separation between the electrodes. In a similar set-up to ours, a detailed analysis which demonstrates the exponential relaxation outside the double layer with a time constant τ was given by Bazant et al. [9]. Clearly in our simulation $l \sim L$. Hence, if one could simulate a system in which the distance between the electrodes is 3 orders of magnitude bigger, as in the experiments, one would obtain also similar relaxation times of the order of 10-100 ms. This observation leads us to believe that our calculations capture qualitatively the dynamics around the particle correctly, at least in times that directed electrophoretic motion is dominant over the Brownian motion ($t <$ 20 ms in Fig. 3).

Discussion

The measurements presented in the experimental section were mainly performed to demonstrate the technical feasibility of continuously monitoring electrophoretic mobility on a single nanoparticle using our nanoCET platform. We are not claiming to be the first group who has measured electrophoretic mobility on a single nanoparticle. To our knowledge, however, no qualitatively similar measurement have been performed on similarly small single nanoparticles for such a long period of time and with such a high

recording speed. Such mobility measurements have been done frequently in the past, in different geometries using fluorescence microscopy. The most remarkable experimental platform in our view is the anti-Brownian electrokinetic (ABEL) trap developed by Cohen and Moerner [10], which is able to measure the transient mobility of single proteins down to 1 nm in size and even a single fluorescent dye molecule. Inherent reliance of the ABEL trap on fluorescence signal, however, limits the time-resolution and maximum duration of tracking a single particle in that platform. In 2014, Wang and Moerner [11] have used a much optimized ABEL trap to extract both mobility and diffusivity of a single protein with a time resolution of 200 ms using time-stamped single photon counting. Despite these outstanding achievements, the time resolution of such measurements in the ABEL trap is hard to improve further because the photon flux is strictly limited by the fluorescence emission rate and the imperfect collection efficiency [12]. Furthermore, because of photo-bleaching of the fluorescent labels, the maximum duration of those measurements are usually less than a few seconds.

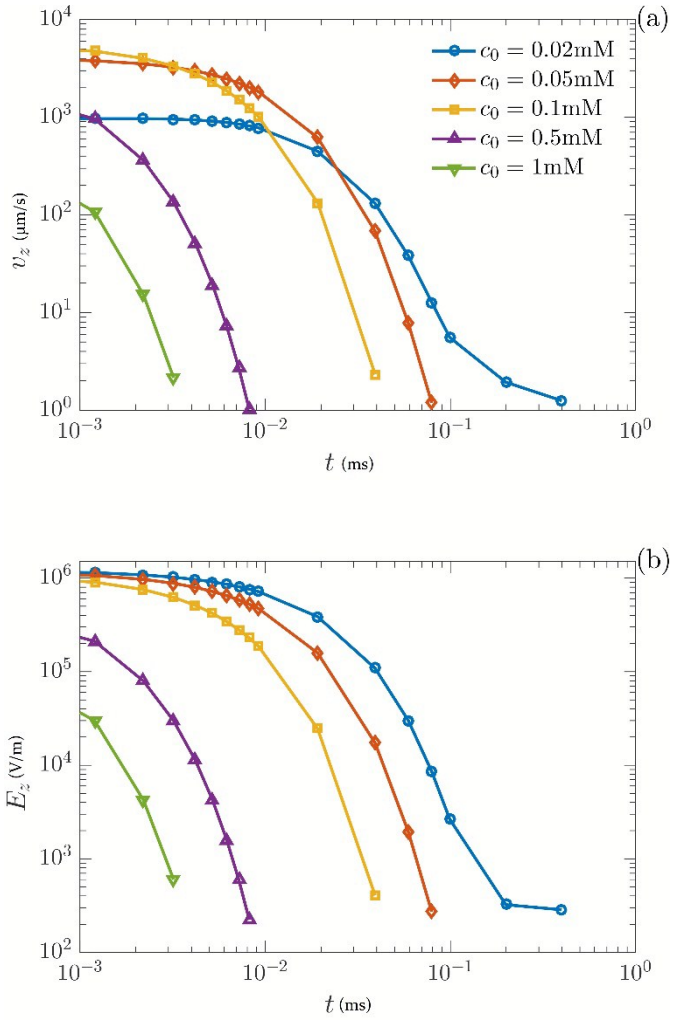

Figure 6: (a) The axial component of the fluid velocity and (b) the axial component of the electric field at the pore centre as a function of time for various bulk salt concentrations c_0. Both quantities decay exponentially except for $c_0 = 0.02$ mM. The relaxation time increases with decreasing salt concentration.

Using the scattering signal on a remarkably low background in the nanoCET platform is the key improvement over previous methods that will allow enhancement of time resolution and extension of measurement duration to a level that one can go beyond transient mobility measurements and monitor the charge kinetics on a single nanoparticle. To reach this goal however, certain improvements have to be made on our current setup, which we discuss here.

We consider a spherical particle as a model system for our discussion. As a typical example, we take a negatively charged colloidal particle with a radius of $a = 5$ nm and a typical surface potential of $\psi_s = -25$ meV in 1 mM (1:1) aqueous electrolyte solution. For this system, the dimensionless size parameter $a/\lambda_D \approx 0.5$. Using the well-known relation $q_s = \epsilon\psi_s(1/\lambda_D + 1/a)$ for surface charge density in this geometry, the total surface charge of the particle is determined to be $Q \approx -10e$ with e the fundamental charge. Using the Smoluchowski relation, the electrophoretic mobility of this particle $\mu \approx 1.8 \times 10^{-8}$ in SI units. Applying the Henry's correction factor is not necessary for the current discussion and we consider the zeta potential has the same value as the above mentioned surface potential. The particle drift velocity under a realistic (unscreened) electric field of 100 kV/m is 1.8 μm/ms. This drift velocity can be measured in our current nanoCET setup with an accuracy better than 1 part in 20. This sensitivity translates to sensing surface charge variations as small as $e/2$ or surface potential change of $k_BT/20$, with a time resolution of 1 ms.

Because electrophoretic mobility in this regime depends only on the surface potential and is independent of the particle size, measuring smaller particles is just a quest of enhancing the optical signal. In future experiments, we expect to achieve more than a 100 fold increase in optical sensitivity by using holographic background reduction. This will allow us to monitor changes in electrophoretic mobility of some large proteins such as fibrinogen, catalase or hemoglobin, and short DNA strands. The scattering signal from smaller molecules can be enhanced by using fluorescent labels for enhancing the particle polarisability due to their large near-resonant dipole moments. As a benchmark, it is worth noting that the polarisability of a single Rhodamine 6G molecule, excited on the red side of its absorption line, is comparable with that of a latex particle of 10 nm in diameter or a gold nanocluster of 5 nm in size that is frequently used as a contrast agent for electron microscopy.

Our numerical modelling demonstrates that the electric field inside the channel is spatially uniform. The exact temporal behavior can be simulated in an up-to-scale model, which requires larger computational resources, or be measured on calibrated tracer particles. The result can then be used to determine the unknown mobility of the particles under investigation. The radial variation of the background fluid motion poses a greater challenge for determining the mobility since it adds extra noise to particle velocity measurements. This noise is more prominent for faster readouts because the particle does not get enough time to sample the whole cross-section of the channel. To correct for this noise, we can implement a three dimensional spatial localization protocol to perform a point by point background flow correction.

Conclusions

In summary, we have investigated the feasibility of performing electrophoretic mobility measurements on individual nanoparticle in

a closed aqueous environment with numerical simulations and proof-of-concept experiments. We have proposed a new tracking experiment, nanoCET, based on a nanocapillary optical fiber platform combined with high speed actuation and readout. This measurements can be readily performed on high refractive index metallic particles as small as 10 nanometers. For measuring smaller particles such as biomolecules, directly, one needs to enhance the optical readout sensitivity, which can be achieved by interferometry. The electrophoretic mobility of particles can be extracted at high measurement rates of several kHz. For such high rates three dimensional localization and careful consideration of the background fluid flow is necessary. Using numerical simulations of PNP-Stokes equation on a smaller model system, we have presented the qualitative behavior of the fluid flow, charge screening, and electric field inside the capillary as a function of time. Our numerical results qualitatively agree with our measurements, but also prove that a true scale calculation with larger computational resources is necessary for quantitatively describing the experiments.

Acknowledgements

S.F. thanks Michel Orrit for hosting the experiment during an early stage of this project and Emiel Wiegers for technical support. This work is financially supported by the European Research Council, Project No. 279248. S.S. acknowledges funding from the European Union's Horizon 2020 under the Marie Skłodowska-Curie grant agreement No. 656327.

Notes and references

1 N.M. Mar, E. R. Lee, G. R. Fleming, B. C. K. Casey, M. L. Perl, E. L. Garwin, C. D. Hendricks, K. S. Lackner, G. L. Shaw, *Phys. Rev. D,* 1996, **53**, 6017–6032.
2 F. Beunis, F. Strubbe, K. Neyts, D. Petrov, *Phys. Rev. Lett.,* 2012**, 108**, 016101.
3 I. Gitlin, J. D. Carbeck, G. M. Whitesides, *Angewandte Chemie Int. Ed*., 2006, **45**, 3022-3060.
4 S. Faez, Y. Lahini, S. Weidlich, R. F. Garmann, K. Wondraczek, M. Zeisberger, M. A. Schmidt, M. Orrit, V. N. Manohoran, *ACS Nano*. 2015, **9** (12), 12349
5 J. H. Masliyah, S. Bhattacharjee, *Electrokinetic and Colloid Transport Phenomena*, John Wiley & Sons 2006, DOI: 10.1002/0471799742
6 J. Gunning, D. Y. C. Chan, and L. R. White, *J. Colloid Interface Sci*., 1995, **170**, 522
7 M. Scott, R. Paul, and K. V. I. S. Kaler, *J. Colloid Interface Sci.,* 2000, **320**, 377
8 A. D. Hollingsworth and D. A. Saville, *J. Colloid Interface Sci.,* 2003, **257**, 65.
9 M. Z. Bazant, K. Thornton, A. Ajdari, *Phys. Rev. E*, 2004, **70**, 021506
10 A. E. Cohen, W. E. Moerner, *Proc. Nat. Ac. Sci.,* 2006, **103**, 4362–4365
11 Q. Wang, W. E. Moerner, Nat. Methods, 2014, **11**, 555–558.
12 M. Kumbakhar, D. Hähnel, I. Gregor, J. Enderlein, *Pramana - J Phys*, 2014, **82**, 121–134.